Superionic behaviour in copper (I) iodide at elevated pressures and temperatures

1998 J. Phys.: Condens. Matter 10 10941

(http://iopscience.iop.org/0953-8984/10/48/015)

J. Phys.: Condens. Matter **10** (1998) 10941–10954. Printed in the UK PII: S0953-8984(98)96843-6

Superionic behaviour in copper (I) iodide at elevated pressures and temperatures

S Hull†, D A Keen†, W Hayes‡ and N J G Gardner†‡

† The ISIS Facility, Rutherford Appleton Laboratory, Chilton, Didcot, Oxfordshire OX11 0QX, UK

‡ The Clarendon Laboratory, Parks Road, Oxford, Oxfordshire OX1 3PU, UK

Received 18 August 1998

Abstract. The structural properties of copper (I) iodide have been investigated at elevated pressures and temperatures using the neutron powder diffraction technique, to probe the effects of pressure on the superionic properties of this compound. On increasing temperature at a pressure of $p = 1.30(8)$ GPa, three structural phase transitions are observed. The first is from the ambient temperature zincblende structured phase CuI-III to rhombohedral CuI-IV at $T = 444(6)$ K. There is only limited cation disorder in CuI-IV which increases gradually with temperature. The preferred locations of the interstitial cations are sites between the tetrahedral and octahedral interstices within the slightly distorted face-centred cubic (f.c.c.) anion sublattice. A subsequent transition to the disordered f.c.c. structured phase CuI-I (α-CuI) occurs at $T = 694(5)$ K. This phase shows complete cation disorder at all measured pressures and temperatures. Finally, CuI undergoes a further phase transition at a temperature of $T = 920(15)$ K. The first diffraction studies of this high pressure phase (labelled CuI-VII) are presented, which indicate that this phase is a body-centred cubic (b.c.c.) superionic with complete disorder of the cation sublattice. The cations are found to preferentially occupy the tetrahedral sites, in a manner similar to that in isostructural (ambient pressure) superionic phases such as α-AgI and α-CuBr. The structural systematics of the superionic binary halide compounds and their thermally induced disorder are briefly summarized.

1. Introduction

At ambient conditions, the three copper (I) halides CuCl, CuBr and CuI all adopt the cubic zincblende structure (space group $F\bar{4}3m$). Together with AgI, they form a family of four tetrahedrally co-ordinated 'I–VII' compounds whose structural behaviour has been extensively investigated as a function of both pressure [1–5] and temperature [6–10]. On increasing pressure at ambient temperature, all four compounds transform to the rocksalt structure (space group $Fm\bar{3}m$) [2–4], though this is somewhat distorted towards fivefold co-ordination in the case of CuI and the true space group is $Cmcm$ [5]. Furthermore, in all four compounds the pressure induced transformation from tetrahedral (zincblende) to octahedral (rocksalt) co-ordination occurs via a number of intermediate phases of lower symmetry [2–4] which have attracted considerable attention as tests of theoretical modelling techniques [11] and for comparison with the high pressure behaviour of the more covalently bonded II–VI and III–V analogues [12–15].

On increasing temperature at ambient pressure, CuI, CuBr and AgI all form superionic phases, which are characterized by extremely high values of ionic conductivity ($\sigma \sim 0.1$–$1\ \Omega^{-1}\ \mathrm{cm}^{-1}$), which are comparable to the liquid state [16]. In the accepted structural

0953-8984/98/4810941+14$19.50

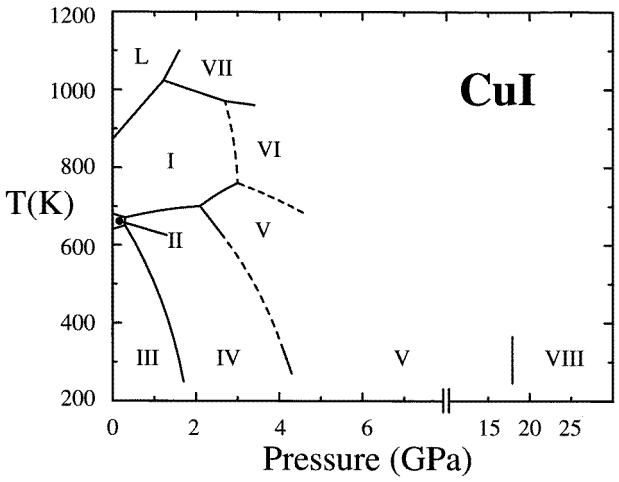

Figure 1. The p–T phase diagram of CuI, principally determined by the DTA measurements of Rapoport and Pistorius [22] . The notation for the various phases is taken from the review by Merrill [29].

model for the superionic phases in these compounds, the cations undergo rapid hops between the interstitial interstices formed by an essentially rigid anion sublattice. In the case of α-AgI [6, 7] and α-CuBr [8], this anion sublattice is body-centred cubic (b.c.c.), whereas it is face-centred cubic (f.c.c.) in α-CuI [8, 10]. In contrast, CuCl only adopts a high temperature superionic phase at pressures greater than $p \sim 0.3$ GPa, forming the b.c.c. structured phase CuCl-III [17]. A long-running debate has focused on the question of which interstitial sites are occupied by the mobile cations. In the b.c.c. structured superionic phases (α-AgI, α-CuBr and CuCl-III) neutron diffraction studies indicate that diffusion occurs between the tetrahedrally co-ordinated sites, probably via the trigonal ones and with little or no occupancy of the octahedral sites [6–8, 10]. However, the situation in the f.c.c. structured phase α-CuI is more controversial, with conflicting evidence for occupancy of the octahedral sites from EXAFS studies [18] and tetrahedral sites from neutron diffraction investigations [10]. Furthermore, molecular dynamics studies have also failed to resolve this question, with recent publications providing different conclusions regarding the occupancy of the octahedral interstices [19–21].

The p–T phase diagram of CuI (see figure 1) determined by DTA measurements [22] is remarkably complex and on increasing pressure at ambient temperature the compound transforms from the zincblende structured phase CuI-III (γ-CuI) to the rhombohedral phase CuI-IV at $p \sim 1.7$ GPa (space group $R\bar{3}m$), to the tetragonal phase CuI-V at $p \sim 4.5$ GPa (space group $P4/nmm$) and to the orthorhombic distorted rocksalt structure in phase CuI-VIII at $p \sim 17$ GPa (space group $Cmcm$) [4, 5]. On increasing temperature at ambient pressure, CuI transforms to the hexagonal phase CuI-II (β-CuI) at $T \sim 645$ K though, under some circumstances, the III $\rightarrow$ II transition is accompanied by the transient appearance of phase CuI-IV [9]. The structure of phase CuI-II was originally proposed to be wurtzite (space group $P\bar{6}_3mc$) [8] but the space group was later assigned to be $P\bar{3}m1$ with significant, though not complete, cation disorder [9]. The transition to the superionic phase CuI-I(α-CuI) occurs at $T \sim 675$ K [10]. No structural information exists concerning phases CuI-VI and CuI-VII.

In this paper we present the results of a powder neutron diffraction study of CuI at pressures of $p = 0.85(5)$ GPa and $p = 1.30(8)$ GPa and at temperatures up to $T = 966(6)$ K. The three major issues to be addressed are the nature of any structural disorder within the rhombohedral phase CuI-IV, the effect of pressure on the disorder mechanism within the superionic phase CuI-I and the structure of (and possible disorder within) phase CuI-VII.

2. Experimental details

Commercially available CuI powder supplied by the Aldrich Chemical Company of stated purity 99.9% was used in these experiments. After grinding, the material was compressed into a 0.1 mm wall thickness cylindrical platinum can of volume $\sim$0.8 cm^3 using a pressure of 0.2 GPa, such that the sample density was close to its theoretical value. The filled can was loaded into a high pressure, high temperature cell which is optimized for time-of-flight neutron diffraction at pressures to $p \sim 1.5$ GPa and temperatures to $T \sim 1200$ K. A detailed description of this device can be found elsewhere [23]. The diffraction experiments principally used the detector banks covering the scattering angle ranges $85^\circ < \pm 2\theta < 95^\circ$ situated on the Polaris high intensity powder diffractometer at the ISIS spallation neutron source, Rutherford Appleton Laboratory, UK [24]. The resultant diffraction data covered the d-spacing range of $0.4 < d$ (Å) < 3.7 with essentially constant resolution of $\Delta d/d \sim 0.6\%$.

Typical counting times were $\sim\frac{1}{2}$ hour for measurements requiring only lattice parameter values and/or phase identification but significantly longer exposures (6 to 12 h) were required to collect diffraction data of sufficient statistical quality to allow full structural refinement, including probing the nature of the thermally induced lattice disorder. The diffraction data were corrected by subtraction of the scattering measured from an empty platinum can inside the pressure cell at a 'typical' temperature of 745 K and for the effects of attenuation of the neutron beam as it passes through the various cell components [23]. Time-of-flight Rietveld refinements of the powder diffraction data used the program TF12LS [25] and its multiphase derivative, which are based on the Cambridge crystallographic subroutine library [26]. The quality of the fit to the experimental diffraction data was assessed using the normal χ^2 statistic defined as $\chi^2 = R_{wp}^2/R_{exp}^2$, where the weighted profile R-factor, R_{wp}, is given by

$$R_{wp}^2 = \sum_{N_d} \frac{(y_{obs} - y_{calc})^2}{(\sigma y_{obs})^2} \Bigg/ \sum_{N_d} \frac{(y_{obs})^2}{(\sigma y_{obs})^2}$$

and the summations are made over the N_d data points used in the fit. The expected R-factor, R_{exp} is then given by

$$R_{exp}^2 = (N_d - N_p) \Bigg/ \sum_{i=1}^{N_d} \frac{(y_{obs})^2}{(\sigma y_{obs})^2}$$

where N_p is the number of fitted parameters. y_{obs} and y_{calc} are the observed and calculated intensities, respectively, and σy_{obs} is the estimated standard deviation on y_{obs} derived from the counting statistics.

3. Results

A qualitative overview of the structural behaviour of CuI on increasing temperature at elevated pressure is shown by the evolution of the neutron powder diffraction patterns at $p = 1.30(8)$ GPa (figure 2). CuI is seen to undergo three first-order structural phase

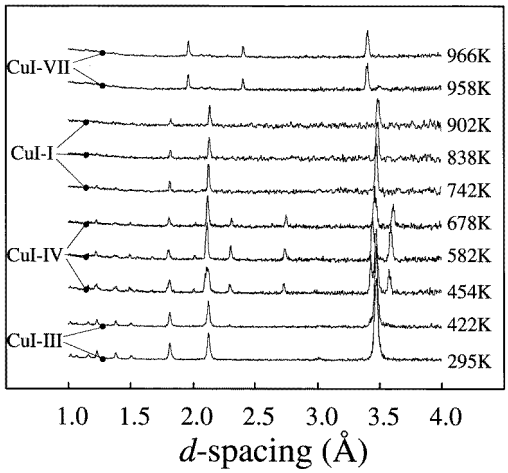

Figure 2. The evolution of the neutron diffraction pattern collected from CuI as a function of increasing temperature at $p = 1.30(8)$ GPa. The sequence of structural phase transitions CuI-III $\rightarrow$ CuI-IV $\rightarrow$ CuI-I $\rightarrow$ CuI-VII is clearly illustrated.

transitions which, with reference to the p–T phase diagram (figure 1), can be identified as the transition from zincblende structured CuI-III to rhombohedral CuI-IV at $T \sim 440$ K, then to the f.c.c. structured CuI-I at $T \sim 695$ K and finally to phase CuI-VII at $T \sim 920$ K. The analysis of the neutron diffraction data collected from the three high temperature phases (CuI-IV, CuI-I and CuI-VII) and its implications for structural disorder are discussed more fully in the following three subsections.

3.1. Phase IV of CuI

The crystal structure of phase CuI-IV has been described by Hull and Keen [3] and its relationship to the structures adopted at ambient pressure (zincblende) and at higher pressure (CuI-V) have also been discussed [4]. As illustrated in figure 3, CuI-IV is rhombohedral, space group $R\bar{3}m$. In the hexagonal description, there are two symmetry independent iodine ions, I1 and I2, situated in the 3(a) sites at $0, 0, 0$ etc and the 3(b) sites at $0, 0, \frac{1}{2}$ etc, respectively. These form a slightly distorted f.c.c. arrangement. The copper ions are located on the 6(c) sites at $(0, 0, z_{Cu})$ etc, with $z_{Cu} \sim \frac{1}{8}$ and thus occupy half the tetrahedral holes formed by the f.c.c. anion sublattice. The structure can then be considered as a three dimensional packing of CuI_4 tetrahedra which share both corners and edges [4].

To date, the structural studies of phase CuI-IV have been performed at elevated pressures and ambient temperature [3, 4] and at ambient pressure and high temperature [10]. In the latter, only limited crystallographic information could be determined because CuI-IV is observed as a transient phase during the sluggish CuI-III $\rightarrow$ CuI-II transformation. We here investigate the evidence for possible thermally induced disorder within this phase as temperature is increased under pressure. We adopt the same approach as in previous studies [9, 10, 17], fitting two datasets measured at $T = 566(3)$ K and $T = 614(3)$ K at $p = 0.85(5)$ GPa using different structural models and assessing their quality using the χ^2 statistic defined above. The results of this procedure are summarized in table 1. The simplest model (A) contains no structural disorder and corresponds to the fully ordered arrangement determined at ambient temperature in previous studies [3] with harmonic thermal vibrations

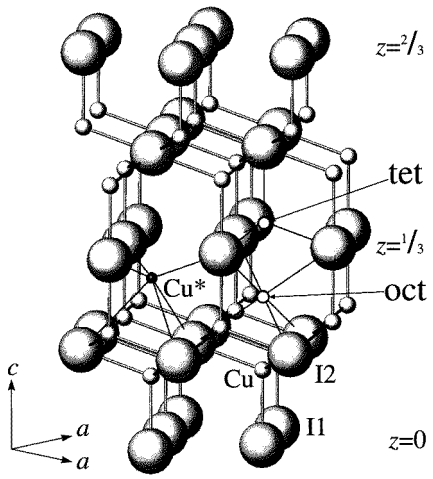

Figure 3. Schematic diagram of the rhombohedral structure of phase CuI-IV. The locations of the tetrahedral and octahedral interstices within the (slightly distorted) f.c.c. anion sublattice are shown. The preferred site for the interstitial cations, Cu^*, is displaced away from the octahedral position towards the anion layer at $z = \frac{1}{3}$.

Table 1. Summary of the structural models used to fit the experimental diffraction data for phase CuI-IV collected at $p = 0.85(5)$ GPa and at $T = 566(3)$ K and $T = 614(3)$ K. The quality-of-fit parameter χ^2 is defined in section 2.

		χ^2	
Model	Description	566(3) K	614(3) K
A	Fully ordered cations	1.51	1.68
B	Random cation interstitials	1.49	1.31
C	Cation interstitials on tetrahedral sites ($z_{Cu^*} = \frac{3}{8}$)	1.49	1.28
D	Cation interstitials on octahedral sites ($z_{Cu^*} = \frac{1}{4}$)	1.50	1.67
E	As C and D but with position z_{Cu^*} variable	1.22	1.20

of both ion species. This gives a modest fit to the data, with significant differences between the measured and calculated intensities of several intense Bragg peaks. In the cubic phases CuI-III and CuI-I, the cation thermal vibrations are known to be anharmonic, being, on average, displaced from the tetrahedral site in a direction away from the nearest neighbour anion. Attempts to describe the cation thermal displacements in the rhombohedral phase CuI-IV did not provide any significant improvement to the quality of the fit and were not considered further.

Model B permits the possibility of Cu^+ disorder by allowing the occupancy of the cation site to vary. This model makes no assumptions concerning the locations of the 'displaced' cations (which we denote by the label Cu^*) and is, as a consequence, physically unrealistic. However, a significant reduction in both χ^2 and the lattice cation (Cu) site occupancy are indications of likely disorder and justify the testing of structurally more complex models (containing more fitted parameters) which explicitly include the locations of the cation interstitials. The next two models constrain the Cu^* interstitials to lie on the remaining tetrahedral sites formed by the f.c.c. anion sublattice, in 6(c) sites at $0, 0, z_{Cu^*}$ etc with $z_{Cu^*} = \frac{3}{8}$ (model C) or on the octahedral sites, in 6(c) sites with $z_{Cu^*} = \frac{1}{4}$ (model D).

Table 2. Results obtained by the least-squares fit of model E to the experimental diffraction data for phase CuI-IV collected at $p = 0.85(5)$ GPa and at $T = 566(3)$ K and $T = 614(3)$ K. Definitions of the various symbols are given in section 3.1.

Phase	CuI-IV	
Space group	$R3m$	
p (GPa)	0.85(5)	
T (K)	566(3)	614(3)
Lattice parameters		
a (Å)	4.2271(5)	4.2466(4)
c	20.919(8)	20.934(9)
c/a	4.9488(2)	4.9295(2)
V/Z (Å^3)	53.95(2)	54.49(2)
Anions		
I1 in 3(a) @ 0, 0, 0 etc	$B_{I1} = 2.4(4)$ Å^2	$B_{I1} = 2.7(3)$ Å^2
I2 in 3(b) @ 0, 0, 1/2 etc	$B_{I2} = B_{I1}$	$B_{I2} = B_{I1}$
Cations		
Cu in 6(c) @ 0, 0, z_{Cu} etc	$B_{Cu} = 4.2(8)$ Å^2	$B_{Cu} = 4.3(9)$ Å^2
Cu* in 6(c) @ 0, 0, z_{Cu^*} etc	$B_{Cu^*} = B_{Cu}$	$B^*_{Cu} = B_{Cu}$
	$z_{Cu} = 0.129(1)$	$z_{Cu} = 0.129(2)$
	$z_{Cu^*} = 0.290(2)$	$z_{Cu^*} = 0.293(3)$
	$m_{Cu} = 0.900(8)$	$m_{Cu} = 0.873(7)$
	$m_{Cu^*} = 0.100(8)$	$m_{Cu^*} = 0.127(7)$

Models C and D both include the constraint that the total number of cations per hexagonal unit cell is six but, with reference to table 1, neither produces a significant improvement in the quality of fit. Similarly, attempts to include both tetrahedral and octahedral interstitial sites simultaneously proved unsuccessful. In the final stage of the analysis, models C and D were adapted to allow the z_{Cu^*} positional parameter to vary away from the centre of the tetrahedral and octahedral cavities. This produced a marked improvement in χ^2 for both datasets (model E in table 1) and gave a stable minimum in χ^2. As shown in table 2, the values of the two positional parameters z_{Cu} and z_{Cu^*} are the same at each temperature to within their estimated standard deviation. With reference to table 2, we also conclude that there is significant thermally induced disorder within CuI-IV, with values of the Cu* site occupancy $m_{Cu^*} = 0.100(8)$ at $T = 566(3)$ K and $m_{Cu^*} = 0.127(7)$ at 614(3) K. The preferred interstitial site is illustrated in figure 3 and is close to the octahedral position but displaced along the c-axis towards the empty tetrahedral sites such that $z_{Cu^*} = 0.29$.

A subsequent series of measurements was performed at a higher pressure of $p = 1.30(8)$ GPa to investigate the effect of temperature on the unit cell shape and volume. These datasets were collected in relatively short times (∼1–2 h) and used to determine the variation of the unit cell constants a and c, the isotropic thermal vibration parameters B_{Cu} and B_I and the extent of cation disorder, m_{Cu^*}. However, these runs were not of sufficient statistical quality to determine the behaviour of the positional parameters z_{Cu} and z_{Cu^*} and these were fixed at values of 0.129 and 0.290, respectively. This procedure is justified by the absence of any significant changes in their values determined in the longer runs (table 2). The results of these measurements are shown in figures 5–8 and will be discussed further in section 4.3.

3.2. Phase I of CuI (α-CuI)

The ambient pressure structure of phase CuI-I has $Fm\bar{3}m$ symmetry [8, 10]. The anions are located in 4(a) sites at 0, 0, 0 etc and form an ideal f.c.c. sublattice. Neutron diffraction

studies at ambient pressure have shown that the four cations per unit cell are randomly distributed over the eight tetrahedral interstices [10]. However, the effect of anharmonic thermal displacements is to shift the time-averaged location of the Cu^+ from the 'ideal' 8(c) positions at $\frac{1}{4}, \frac{1}{4}, \frac{1}{4}$ etc (which lie at the centre of the I_4 tetrahedra) into 32(f) sites at x_{Cu}, x_{Cu}, x_{Cu} etc with $x_{Cu} \sim 0.29$. There have been conflicting reports that a fraction of the cations are also located on octahedral 4(b) positions at $\frac{1}{2}, \frac{1}{2}, \frac{1}{2}$ etc [18, 21].

Least-squares refinements of the time-averaged structure of CuI-I at elevated pressure used data collected at five temperatures in the range $T = 710(5)$ K to $T = 934(6)$ K at $p = 1.30(8)$ GPa. These results are summarized in table 3. Starting models based on the ambient pressure structure described above, with all Cu^+ on 32(f) sites provided excellent fits to all the datasets, with $\chi^2 \sim 1.1$–1.3. In common with the ambient pressure data, the refined values x_{Cu} are indicative of considerable anharmonic vibrations of the Cu^+. Attempts to improve the quality of the fit further by allowing a fraction of the cations to 'move' from the tetrahedral holes to the octahedral 4(b) sites proved unsuccessful, with unstable minimization of χ^2. Similarly, there is no evidence for non-random occupancy of the tetrahedral interstices if, for example, the cations preferentially filled only four of the available eight positions. Physically, the latter would be considered as a tendency towards the (lower symmetry) structures adopted by the lower temperature phases CuI-I and CuI-IV. There is, therefore, no evidence to suggest changes in the ionic conductivity mechanism within phase CuI-I at pressures up to $p = 1.30(8)$ GPa. Least-squares refinements of the data determined the values of cubic unit cell constant a, isotropic thermal vibration parameters B_{Cu} and B_I and the single positional parameter x_{Cu} (table 3).

3.3. Phase VII of CuI

On increasing temperature above the CuI-I phase at a pressure $p = 1.30(8)$ GPa, additional weak diffraction peaks are observed at $T = 910(6)$ K. On further heating to $T = 950(6)$ K all the peaks corresponding to CuI-I disappear. This structural transition occurs at a

Table 3. Results obtained by the least-squares fit to the experimental diffraction data for phase CuI-I collected at $p = 1.30(8)$ GPa and at $T = 710(5)$ K to $T = 934(6)$ K. Definitions of the various symbols are given in section 3.2. The quality-of-fit parameter χ^2 is defined in section 2.

Phase			CuI-I		
Space group			$Fm\bar{3}m$		
p (GPa)			1.30(8)		
T (K)	710(5)	742(3)	838(3)	902(3)	934(6)
Lattice parameters					
a (Å)	6.004(1)	6.011(2)	6.028(2)	6.039(2)	6.043(3)
V/Z (Å^3)	54.108(9)	54.30(2)	54.76(2)	55.06(2)	55.17(3)
Anions					
I in 4(a) @ 0, 0, 0 etc	$B_I = 4.6(8)$ Å^2	$B_I = 5.1(7)$ Å^2	$B_I = 5.5(5)$ Å^2	$B_I = 5.6(5)$ Å^2	$B_I = 6.0(6)$ Å^2
Cations					
Cu in 32(f) @	$x_{Cu} = 0.297(4)$	$x_{Cu} = 0.291(5)$	$x_{Cu} = 0.286(7)$	$x_{Cu} = 0.290(4)$	$x_{Cu} = 0.300(4)$
x_{Cu}, x_{Cu}, x_{Cu}	$m_{Cu} = \frac{1}{8}$ (fixed)	$m_{Cu} = \frac{1}{8}$ (fixed)	$m_{Cu} = \frac{1}{8}$ (fixed)	$m_{Cu} = \frac{1}{8}$ (fixed)	$m_{Cu} = \frac{1}{8}$ (fixed)
etc	$B_{Cu} = 6.0(7)$ Å^2	$B_{Cu} = 6.8(8)$ Å^2	$B_{Cu} = 7.0(7)$ Å^2	$B_{Cu} = 7.5(7)$ Å^2	$B_{Cu} = 8.1(6)$ Å^2
Quality-of-fit					
χ^2	1.12	1.21	1.20	1.28	1.14

significantly lower temperature than the CuI-I $\rightarrow$ CuI-VII one observed in the DTA studies of Rapoport and Pistorius [22] at $T \sim 1050$ K. However, in view of the inherent uncertainties in the temperature calibration within pressure cells we believe that the two transitions are the same and assign the new diffraction pattern to phase CuI-VII (see figure 1).

The observed diffraction pattern of CuI-VII contains only three intense Bragg peaks at d-spacings of $d = 1.96$, 2.40 and 3.40 Å, with a further three weak reflections seen at lower values of d (figure 2). These can be indexed on a body centred cubic unit cell with lattice parameter $a \sim 4.80$ Å. The relatively weak intensities of the Bragg peaks and the presence of significant coherent diffuse scattering observed as undulations in the measured 'background' between the Bragg peaks are indicative of a highly disordered ionic arrangement. By analogy with the b.c.c. structured superionic phases α-AgI [6, 7] and α-CuBr [8], we place two anions in the 2(a) Wyckoff sites of space group $Im\bar{3}m$ at $0, 0, 0$ and $\frac{1}{2}, \frac{1}{2}, \frac{1}{2}$. To determine the time-averaged locations of the cations we follow the procedure adopted previously [17] and consider structural models which distribute the Cu^+ over the possible interstices formed by the b.c.c. anion sublattice. These are illustrated in figure 4 and the results are summarized in table 4.

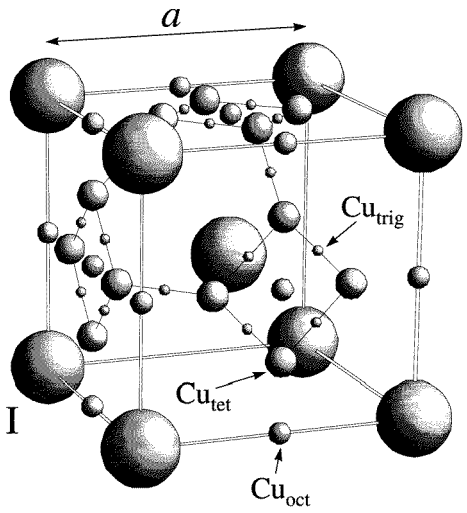

Figure 4. Schematic diagram of the b.c.c. structure of superionic phase CuI-VII. The locations of the octahedral (Cu_{oct}), tetrahedral (Cu_{tet}) and trigonal (Cu_{trig}) interstices are shown. The lines joining the tetrahedral sites represent the proposed Cu^+ diffusion path within the superionic phase of isostructural α-AgI [6, 7].

Table 4. Summary of the structural models used to fit the experimental diffraction data for phase CuI-VII collected at $p = 1.30(8)$ GPa and at $T = 966(6)$ K. The quality-of-fit parameter χ^2 is defined in section 2.

Model	Description	χ^2
A	b.c.c. anions, cations in 6(b) octahedral sites	1.62
B	b.c.c. anions, cations in 12(d) tetrahedral sites	1.28
C	b.c.c. anions, cations in 24(h) trigonal sites	1.44
D	b.c.c. anions, cations in 12(d) and 24(h) sites	1.29

Table 5. Results obtained by the least-squares fit of model B to the experimental diffraction data for phase CuI-VII collected at $p = 1.30(8)$ GPa and at $T = 966(6)$ K. Definitions of the various symbols are given in section 3.3.

Phase	CuI-VII
Space group	$Im\bar{3}m$
p (GPa)	1.30(8) GPa
T (K)	966(3)
Lattice parameter	
a (Å)	4.7983(4)
V/Z (Å^3)	55.237(5)
Anions	
I in 2(a) @ 0, 0, 0 etc	$B_I = 8.4(6)$ Å^2
Cations	
Cu in 12(d) @ $\frac{1}{4}, \frac{1}{2}, 0$ etc	$B_{Cu} = 13.1(8)$ Å^2
	$m_{Cu} = \frac{1}{6}$ (fixed)

The least-squares refinements to determine the structure of phase CuI-VII used diffraction data collected at $p = 1.30(8)$ GPa and $T = 966(6)$ K. Models A, B and C distribute the cations over the octahedral 6(b) sites at $\frac{1}{2}, \frac{1}{2}, 0$, etc, the tetrahedral 12(d) sites at $\frac{1}{4}, \frac{1}{2}, 0$ etc and the trigonal 24(h) sites at $x, x, 0$ etc with $x = \frac{3}{8}$, respectively. Model A gives a relatively poor fit to the data, with $\chi^2 = 1.62$ and exceptionally large values of the Cu^+ isotropic thermal vibration parameter B_{Cu} ($\sim$25 Å^2). Model B and, to a lesser extent, model C provide adequate fits to the data ($\chi^2 = 1.28$ and 1.44, respectively) with physically meaningful values of the fitted parameters. The final fits to the data used model D, which allows simultaneous occupation of both the tetrahedral and trigonal positions. This description also provides a good fit to the data ($\chi^2 = 1.29$), though not significantly improved over model B and with minimal redistribution of cations from the tetrahedral to the trigonal sites. We therefore conclude that the simplest model which best fits the experimental data for phase CuI-VII is model B, with the fitted parameters listed in table 5. It is, however, important to emphasize that the adopted model considers the structural disorder as instantaneous hops of the Cu^+ between well defined (tetrahedral) crystallographic sites. In reality, the superionic state is a highly dynamic configuration, with a degree of correlation between the mobile ions and significant anisotropic and anharmonic thermal vibrations. The necessity to perform the diffraction measurements at elevated pressures and temperatures and the inherently weak nature of the diffraction intensity provided by such disordered systems restricts the number of Bragg peaks that can be measured. As a result, no attempts to analyse the diffraction data using more complex models are appropriate and none have been considered.

4. Discussion

With the exception of the slightly lower CuI-I $\rightarrow$ CuI-VII transition temperature discussed in section 3.3, the structural phase transitions observed at elevated pressures and temperatures in this work are consistent with the p–T phase diagram of CuI determined previously by DTA methods [22]. As discussed by Salamon [27], the phases CuI-III and CuI-I obey the necessary Landau criteria for a second-order transition [28] and on increasing temperature at ambient pressure a gradual (order $\rightarrow$ disorder) transition of the Cu^+ within the f.c.c.

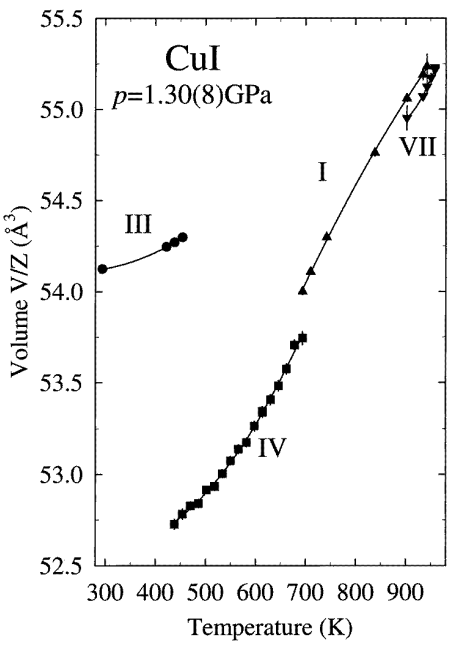

Figure 5. The temperature variation of the unit cell volume per formula unit (V/Z) of CuI at $p = 1.30(8)$ GPa, illustrating the large decrease in volume at the CuI-III $\rightarrow$ CuI-IV transition and the smaller discontinuities at the CuI-IV $\rightarrow$ CuI-I and CuI-I $\rightarrow$ CuI-VII transitions.

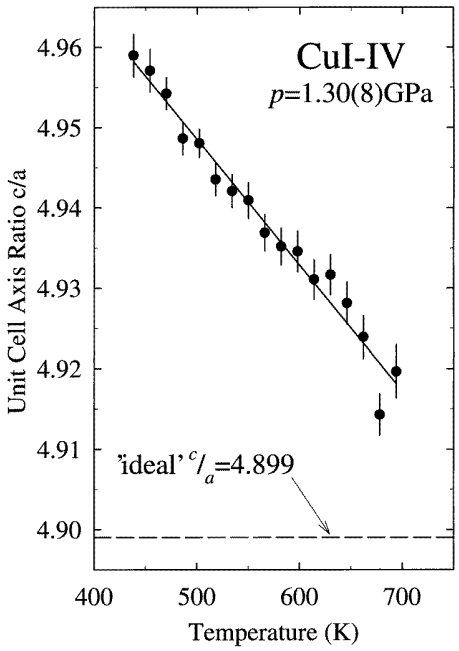

Figure 6. The temperature variation of the unit cell axial ratio c/a for phase CuI-IV at $p = 1.30(8)$ GPa.

anion sublattice might be expected. However, in reality this process is interrupted by the presence of phase CuI-II. The two transitions CuI-III $\rightarrow$ CuI-II and CuI-II $\rightarrow$ CuI-I occur within a narrow temperature range ($\sim$20 K [9]) and are strongly first-order in character because the intermediate phase CuI-II possesses a hexagonal close packed (h.c.p.) anion sublattice. The work presented in this paper confirms that, at pressures in excess of $\sim$0.2 GPa, the intervening hexagonal phase CuI-II is eliminated and the CuI-III $\rightarrow$ CuI-I transformation occurs via the rhombohedral CuI-IV polymorph. In principle, the structural changes on increasing temperature through the CuI-III $\rightarrow$ CuI-IV $\rightarrow$ CuI-I sequence of phases could be continuous, with only a slight distortion of the f.c.c. anion sublattice within phase CuI-IV and a change in the occupancy of the tetrahedral sites from fully ordered (CuI-III) through partially disordered (CuI-IV) to complete disorder (CuI-I). However, as illustrated in figures 5, 7 and 8, there are abrupt changes in the structural properties at the CuI-III $\rightarrow$ CuI-IV and CuI-IV $\rightarrow$ CuI-I transitions, which must be considered to be first order in character. Clearly, molecular dynamics simulations could be valuable in understanding why the stable intermediate phase changes from CuI-II to CuI-IV with increased pressure and in providing important information concerning the nature of the associated transitions.

Figure 5 illustrates the change in unit cell volume per formula unit (V/Z) of CuI as a function of temperature at $p = 1.30(8)$ GPa. The volume change at the CuI-III $\rightarrow$ CuI-IV transition is large $(\Delta V/V = -2.8(1)\%)$, in accord with the behaviour observed on increasing p at ambient temperature and the negative slope of the phase boundary illustrated

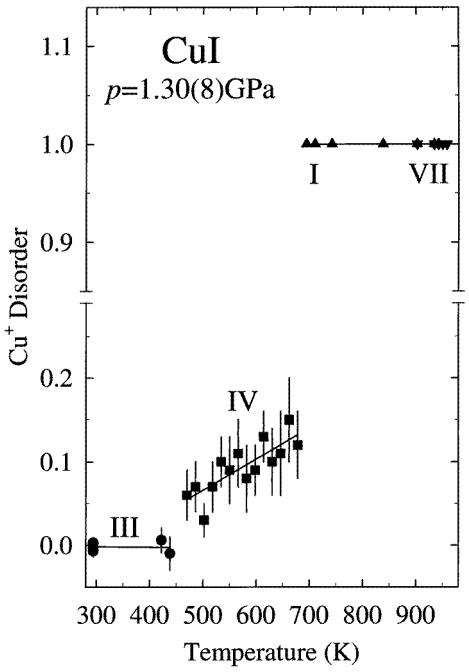

Figure 7. The temperature variation of the Cu^+ disorder within CuI at $p = 1.30(8)$ GPa, illustrating the gradual increase in the partial disorder within the rhombohedral phase CuI-IV.

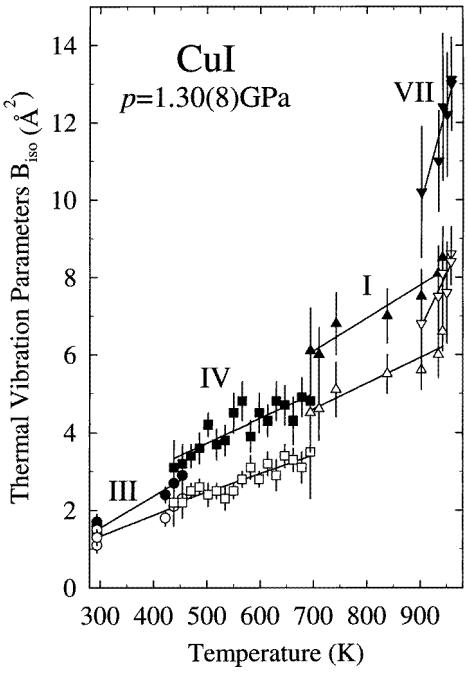

Figure 8. The temperature variation of the isotropic thermal vibration parameters (B_{iso}) of CuI at $p = 1.30(8)$ GPa. The open and closed symbols represent the anions and cations, respectively.

in figure 1. Similarly, the smaller volume changes at the two subsequent transitions ($\Delta V/V = +0.5(1)\%$ for CuI-IV $\rightarrow$ CuI-I and $\Delta V/V = -0.5(1)\%$ for CuI-I $\rightarrow$ CuI-VII) are consistent with the essentially flat phase boundaries.

The following three subsections describe the structural basis of the disorder within each of the three high temperature phases observed at high pressure.

4.1. Phase IV of CuI

As discussed previously [4], the ambient temperature (fully ordered) structure of rhombohedral phase CuI-IV can be straightforwardly derived from the zincblende arrangement (CuI-III) by redistributing the Cu^+ over the available tetrahedral interstices and slightly distorting the f.c.c. anion sublattice by elongating it along one of the threefold axes. The lattice cations located in 6(c) sites at $0, 0, z_{Cu}$ are tetrahedrally co-ordinated to I^-. However, the cations are slightly displaced away from the centre of the tetrahedron, with $z_{Cu} = 0.129(1)$ rather than $z_{Cu} = \frac{1}{8} = 0.125$. In addition, the anion cage is slightly distorted, being elongated along the *c*-axis because the axial ratio c/a (4.92–4.96) is marginally in excess of the ideal value $c/a = 2\sqrt{6} = 4.899$. As illustrated in figure 6, c/a decreases on increasing temperature as the distortion of the anion sublattice away from the perfect f.c.c. arrangement diminishes. The overall effect of the 'non-ideal' values of z_{Cu} and c/a is to produce three Cu-I2 distances of 2.57 Å and a single Cu-I1 one of 2.70 Å, and the angles between these bonds are different ($\angle$I2–Cu–I2 = 111.1° and $\angle$I1–Cu–I2 = 107.8°) but span the ideal tetrahedral value of 109.47°.

As shown in figure 7, CuI-IV displays only partial cation disorder, which increases gradually with increasing temperature. Similar behaviour is observed on increasing temperature within the phase CuI-II at ambient pressure [6]. The increase of the thermal parameters through the phases CuI-IV, CuI-I and CuI-VII, which is shown in figure 8, is also indicative of increased cationic mobility. In view of the strongly layered nature of the structure of CuI-IV (see figure 3), we might expect any structural disorder at elevated temperatures to be somewhat different to that seen in the two high temperature cubic polymorphs, CuI-I and CuI-VII. Analysis of the neutron diffraction data (section 3.1) indicates that the preferred locations for the interstitial cations Cu^* are in 6(c) sites at $0, 0, z_{Cu^*}$, but with $z_{Cu^*} \sim 0.29$ rather than the empty tetrahedral site value of $z_{Cu^*} = \frac{3}{8}$. These cations then have three Cu^*–I1 bond lengths of 2.61 Å and interbond angles $\angle$I1–Cu^*–I1 $= 109.1^\circ$, values very close to those expected for tetrahedral co-ordination. However, the single fourth cation–anion bond is replaced by three longer Cu^*–I2 distances of 3.58 Å, such that the interbond angles are $\angle$I1–Cu^*–I2 $= 85.7^\circ$ and $\angle$I2–Cu^*–I2 $= 72.8^\circ$. As such, the co-ordination geometry around the interstitial Cu^* site can be considered as intermediate between tetrahedral and octahedral. With reference to figure 3, this cation location is a very plausible one, since electrostatic repulsions caused by the Cu^+ layers perpendicular to the *c*-axis favour residence of sites close to the anion layer at $z = \frac{1}{3}$. The cations are presumably unable to sit exactly within this layer because it would involve planar co-ordination to only three anions.

4.2. Phase I of CuI (α-CuI)

As discussed in section 3.2, the neutron diffraction data indicate that pressures up to $p \sim 1.30(8)$ GPa have no measurable effect on the extent of structural disorder within phase CuI-I, with the Cu^+ randomly distributed over the tetrahedral sites formed by the f.c.c. anion sublattice. In particular, the reduction in unit cell volume over this pressure range (by $\sim -7\%$ compared to ambient pressure) does not favour the partial segregation of Cu^+ onto a subset of the tetrahedral sites. This behaviour would represent a tendency towards the zincblende or (ordered) rhombohedral (CuI-IV) structures. Similarly, there is no evidence that pressure favours the occupancy of octahedral sites over tetrahedral ones, despite the fact that the latter are somewhat larger voids within the f.c.c. anion sublattice. (Cu^+–I^- $= a/2$ for the octahedral sites and $\sqrt{3}a/4 = 0.433a$ for the tetrahedral ones). These findings favour the description of the conduction mechanism of CuI proposed by Zheng-Johansson *et al* [19, 20] using molecular dynamics simulations and do not support the work of Ihata and Okazaki [21] (using essentially the same technique) who predict a significant occupancy of the octahedral positions.

4.3. Phase VII of CuI

The description of the b.c.c. structured superionic phase CuI-VII given in section 3.3 indicates that the cations preferentially reside on the tetrahedral sites, with no evidence for significant occupancy of the octahedral positions. This structural model is essentially identical to that found in the ambient pressure b.c.c. superionic phases α-AgI [6, 7] and α-CuBr [8]. When combined with the recent discovery of a similar superionic phase in CuCl at $p = 0.73$ GPa and $T = 740$ K [17], it is now clear that the b.c.c. structure is a common superionic configuration for all four of the 'I–VII' compounds which are tetrahedrally co-ordinated at ambient pressure and temperature. Indeed, the preferred tetrahedral cation locations are the same in all four compounds, despite the differences in anion size and the

degree of covalent/ionic character of the bonding. Since CuI is the most covalent of the four systems it is, perhaps, expected that the tetrahedral occupancy in the b.c.c. structured phase is observed.

5. Conclusions

In the wider context of structural studies of fast-ion conductors, it is clear that measurements performed at elevated pressures can provide useful information by allowing access to different disordered phases so that structural trends can be identified. In both the f.c.c. and b.c.c. structured superionic phases of CuI there is preferential cation occupancy of the tetrahedral sites. This mirrors the behaviour at very high pressures, because the Cu^+ remain tetrahedrally co-ordinated to anions with the anti-litharge structured phase (space group $P4/nmm$ [4]) stable between $p \sim 4.5$ GPa and $p \sim 17$ GPa, and only adopt a distorted fivefold co-ordinated arrangement in the next phase CuI-VIII, with no evidence of octahedral co-ordination up to the maximum pressures studied ($p \sim 40$ GPa [5]). In this context, it is surprising that the cations are not located in the empty tetrahedral sites in the rhombohedral phase CuI-IV. Whilst we can speculate that this is a feature of electrostatic repulsion caused by the layered nature of this phase, it would certainly be interesting to perform molecular dynamics simulations of this phase to probe in detail the unusual diffusion mechanism which must occur. Similarly, the opportunity to perform measurements of the ionic conductivities at high pressures and high temperatures would allow a direct comparison of the degree of the cation mobility within neighbouring f.c.c. and b.c.c. structured phases of the same compound. The latter phase is generally considered to be a 'better' superionic because the number of tetrahedral sites per cation is higher (six compared to two) [18] but a quantitative comparison is, in principle, possible in CuI because the two phases have very similar densities (figure 5).

Acknowledgments

The work presented in this paper forms part of a wider project investigating the high pressure behaviour of superionic conductors funded by the Engineering and Physical Sciences Research Council (reference P:AK:113 C2). One of us (NJGG) is grateful to the Engineering and Physical Sciences Research Council and the Rutherford Appleton Laboratory for financial support during his studentship.

References

[1] Meisalo V and Kalliomäki M 1973 *High Temp.–High Pressure* **5** 663
[2] Keen D A and Hull S 1993 *J. Phys.: Condens. Matter* **5** 23
[3] Hull S and Keen D A 1993 *Europhys. Lett.* **23** 129
[4] Hull S and Keen D A 1994 *Phys. Rev.* B **50** 5868
[5] Hofmann M, Hull S and Keen D A 1995 *Phys. Rev.* B **51** 12 022
[6] Wright A F and Fender B E F 1977 *J. Phys. C: Solid State Phys.* **10** 2261
[7] Nield V M, Keen D A, Hayes W and McGreevy R L 1993 *Solid State Ion.* **66** 247
[8] Bührer W and Hälg W 1977 *Electrochim. Acta* **22** 701
[9] Keen D A and Hull S 1994 *J. Phys.: Condens. Matter* **6** 1637
[10] Keen D A and Hull S 1995 *J. Phys.: Condens. Matter* **7** 5793
[11] Hsueh H C, MacLean J R, Guo G Y, Lee M H, Clark S J, Ackland G J and Crain J 1995 *Phys. Rev.* B **51** 12 216
[12] Chelikowsky J R and Burdett J K 1986 *Phys. Rev. Lett.* **56** 961

[13] Chelikowsky J R 1987 *Phys. Rev.* B **35** 1174
[14] Christensen N E, Satpathy S and Pawlowska Z 1987 *Phys. Rev.* B **36** 1032
[15] Mujica A and Needs R J 1993 *Phys. Rev.* B **48** 17 010
[16] Hayes W 1986 *Contemp. Phys.* **27** 519
[17] Hull S and Keen D A 1996 *J. Phys.: Condens. Matter* **8** 6191
[18] Boyce J B and Huberman B A 1979 *Phys. Rep.* **51** 189
[19] Zheng-Johansson J X M, Ebbsjö I and McGreevy R L 1995 *Solid State Ion.* **82** 115
[20] Zheng-Johansson J X M, Ebbsjö I and McGreevy R L 1996 *Solid State Ion.* **83** 35
[21] Ihata K and Okazaki H 1997 *J. Phys.: Condens. Matter* **9** 1477
[22] Rapoport E and Pistorius C W F T 1968 *Phys. Rev.* **172** 838
[23] Hull S, Keen D A, Done R, Pike T and Gardner N J G 1997 *Nucl. Instrum. Methods* A **385** 354
[24] Hull S, Smith R I, David W I F, Hannon A C, Mayers J and Cywinski R 1992 *Physica* B **180&181** 1000
[25] David W I F, Ibberson R M and Matthewman J C 1992 *Rutherford Appleton Laboratory Report* RAL-92-031
[26] Brown P J and Matthewman J C 1992 *Rutherford Appleton Laboratory Report* RAL-92-032
[27] Salamon M B 1979 *Physics of Superionic Conductors (Topics in Current Physics 15)* ed M B Salamon (Berlin: Springer) p 190 and references therein
[28] Landau L D and Lifschitz E 1968 *Statistical Physics* (New York: Pergamon)
[29] Merrill L 1977 *J. Phys. Chem. Ref. Data* **6** 1205